JOURNAL OF AGRICULTURAL AND FOOD CHEMISTRY

# Molecular Dynamics Study on the Biophysical Interactions of Seven Green Tea Catechins with Lipid Bilayers of Cell Membranes

TIMOTHY W. SIRK,[†] EUGENE F. BROWN,[†] AMADEU K. SUM,*[,‡] AND MENDEL FRIEDMAN[§]

Department of Mechanical Engineering, Virginia Polytechnic Institute and State University, Blacksburg, Virginia 24061, Department of Chemical Engineering, Colorado School of Mines, Golden, Colorado 80401, and Western Regional Research Center, Agricultural Research Service, U.S. Department of Agriculture, Albany, California 94710

Molecular dynamics simulations were performed to study the interactions of bioactive catechins (flavonoids) commonly found in green tea with lipid bilayers, as a model for cell membranes. Previously, multiple experimental studies rationalized catechin's anticarcinogenic, antibacterial, and other beneficial effects in terms of physicochemical molecular interactions with the cell membranes. To contribute toward understanding the molecular role of catechins on the structure of cell membranes, we present simulation results for seven green tea catechins in lipid bilayer systems representative of HepG2 cancer cells. Our simulations show that the seven tea catechins evaluated have a strong affinity for the lipid bilayer via hydrogen bonding to the bilayer surface, with some of the smaller catechins able to penetrate underneath the surface. Epigallocatechin-gallate (EGCG) showed the strongest interaction with the lipid bilayer based on the number of hydrogen bonds formed with lipid headgroups. The simulations also provide insight into the functional characteristics of the catechins that distinguish them as effective compounds to potentially alter the lipid bilayer properties. The results on the hydrogen-bonding effects, described here for the first time, may contribute to a better understanding of proposed multiple molecular mechanisms of the action of catechins in microorganisms, cancer cells, and tissues.

**KEYWORDS: Tea catechins; hydrogen bond; surface binding; molecular dynamics**

## INTRODUCTION

Catechins present in apples, berries, chocolate, grapes, purple potatoes, and teas are reported to be associated with a large number of beneficial health effects. These include antiallergic, anticarcinogenic, anticholesterol, antidiabetic, anti-inflammatory, antihypertensive, antimicrobial, and antineurodegenerative properties, which are reviewed in refs *1*−*3*.

Previously, we reported that green tea gallocatechins and black tea theaflavins exhibited antimicrobial activities at nanomolar levels against the foodborne pathogen *Bacillus cereus*, that the tea catechins without gallate side chains were all inactive, that antimicrobial activities of individual catechins paralleled corresponding activities against human cancer cells (*4, 5*), and that tea catechins reduced levels of *Clostridium perfringens* spore germination and outgrowth during abusive cooling of ground beef, chicken, or pork (*3*). Other investigators reported that antioxidative tea extracts increased the shelf life of beef patties (*6*−*8*), inhibited lipid oxidation in raw beef to a greater extent than did vitamin C (*9*), improved the functionality (lipid oxidation, trapping of free radicals, and sensory properties) (*10*) and degradation of vitamin E in cooked pork patties (*11*), and inhibited the formation of heterocyclic amine carcinogens in meat (*12*).

A catechin can exist as one of two geometrical isomers depending on the stereochemical configuration of the 3′,4′-dihydroxyphenyl and hydroxyl groups at the 2- and 3-positions of the C ring: *trans*-catechins and *cis*-epicatechins. Each of geometric isomers, in turn, exists as two optical isomers: (+)-catechin and (−)-catechin (C) and (+)-epicatechin and (−)-epicatechin (EC), respectively. (−)-Catechin can be modified by esterification with gallic acid to form (−)-catechin-3-gallate (CG), epicatechin-3-gallate (ECG), (−)-epigallocatechin-3-gallate (EGCG), and (−)-gallocatechin-3-gallate (GCG), respectively. There is wide variation in both individual and total catechin contents of widely consumed commercial teas (*13, 14*).

One of several mechanisms by which catechins operate at the cellular−molecular level involves interaction with components of cell membranes leading to prevention of binding of

* To whom correspondence should be addressed. Tel: 303-273-3873. Fax: 303-273-3730. E-mail: asum@mines.edu.
[†] Virginia Polytechnic Institute and State University.
[‡] Colorado School of Mines.
[§] U.S. Department of Agriculture.

10.1021/jf8013298 CCC: $40.75 
Published on Web 08/02/2008

bioactive molecules such as enzymes to receptor sites, a change in membrane potential, and increased permeability for protons and potassium ions. The loss of the ion gradient is responsible for the loss of essential metabolic processes in the cell and consequently cell death (*15*−*18*). For example, long-term drinking of green tea partially prevented adverse changes in the structure and function of rat cell membranes caused by aging and chronic ethanol intoxication (*19*).

Large differences in biological activities of structurally different catechins may to be due to differences in relative affinities to lipid layers of cell membranes. Features of catechins that may influence affinities to cell membranes include stereochemistry structure, the presence of galloyl (gallate ester) side chains, and the number of phenolic OH groups. To place the findings of the present study in proper perspective, we will first summarize the following reported studies designed to define molecular interactions of catechins with lipid bilayers of cell membranes.

Differential scanning calorimetry and spectroscopic studies by Catura et al. (*20*) showed that galloylated catechins ECG and EGCG partitioned efficiently into biological membranes, were located deep in the phospholipid palisade, affected the extent of hydration of the phospholipids−water interface, perturbed the membrane structure, and induced higher amounts of leakage from bacterial model membranes than did the corresponding nongalloylated homologues (+)-C and (−)-EC. EGCG was the most effective of the catechins studied in perturbing the membrane structure of bacteria-like model membranes. In contrast, the nongalloylated catechins presented a shallow location on the membrane close to the phospholipid−water surface.

Results of a study by Lozano et al. (*21*) on electron transfer and hydrogen-donating abilities of EGCG and ECG cysteine derivative suggest that the electron transfer capacity of the entire molecule may be largely responsible for inhibiting the growth of HT29 cancer cells. By contrast, nongalloylated catechin derivatives did not significantly influence the cell cycle or cell death.

Results from solution NMR spectroscopy studies by Ueksa et al. (*22*) showed that ECG and EGCG interact with the choline group located on the surface of lipid membranes, move freely on the surface of the lipid bilayers, and then bind to receptor sites and proteins. Line broadening in the NMR spectra of ECG and EGCG was attributed to the restricted motion of the catechins in the bicelles. Both the B ring and the galloyl moiety of the catechin molecule play important roles in these interactions.

Solid state NMR spectroscopy and related studies by Kajiya and colleagues (*23*−*27*) showed that the amount of tea catechins incorporated in lipid bilayers decreased with increasing negative charge of the bilayers and was competitively affected by the presence of more than one catechin, that EGCG interacts with and moves freely on the membrane surface facilitating its binding to target receptors, that the hydrophobic domain of EGCG protrudes into lipid bilayers and contacts the inner lipophilic regions, and that the intracellular dynamic state of catechins in cell membranes correlates with biological properties.

Atomic orbital energy calculations showed that the EGCG and ECG can act as an electronegative site in inhibiting the enzyme fatty acid synthase that is involved in carcinogenesis. The galloylated catechins were more susceptible to nucleophilic attack by this enzyme than were the nongalloylated ones (*28*).

Phase-contrast fluorescence microscopy showed that EGCG disrupted lipid vesicles, resulting in leakage of the internal fluorescence probe calcein (*29*). The cardioprotective and other beneficial effects of catechins appear to be due to a direct effect on plasma membranes, resulting in a change in membrane fluidity (*18, 30*).

Quantum chemical calculations of reaction rate constants of hydroxyl radical of EGCG showed that hydrogen bonding between the radical part of the B ring of the catechin and a galloyl OH group decreased the bond dissociation energies (BDE) of the phenolic OH group (*31*). A related density functional theory calculation showed that the O−H BDE value was strongly dependent on the hydroxyl position in the benzene rings of simple phenolic acids (caffeic, ferulic, *p*-coumaric, and cinnamic) and the existence of additional interactions due to hydrogen bonding (*32*). Our studies revealed similar large variations in antimicrobial properties of benzaldehydes and benzoic acids substituted with one, two, or three phenolic OH groups on the benzene rings (*33*).

Medina et al. (*34*) showed that catechin gallate and gallocatechin gallate donated 3.8 and 4.0 electrons per mol to lipids of minced fish muscle as compared to 1.7 and 2.3 mol of electrons per mol for catechin and gallocatechin, that catechin was a better inhibitor of oxidation than gallocatechin, that the antioxidative activities of catechin gallate and gallocatechin gallate were similar, that metal-chelating capacities and partitioning between oily and aqueous phases of four catechins did not correlate with antioxidative activities, and that caffeic acid (3,4-dihydroxycinnamic acid) strongly inhibited rancidity in the fish model.

To provide additional insights about the possible role of hydrogen-bonding interactions of structurally different catechins with components of cell membranes, the main objective of the present study was to explore biophysical interactions of the following compounds as they interact with lipid bilayers (model cell membranes) by molecular dynamics simulations: C, EC, EGC, CG, ECG, EGCG, GCG (**Figure 1**). The dynamics of the interactions are interpreted in terms of the following molecular parameters: hydrogen bonding, adsorption/absorption, molecular orientation of stereostructures, and presence/absence of functional groups among the catechins.

## MATERIALS AND METHODS

**Simulation Details.** Molecular dynamics were performed for each of the seven catechins with a lipid bilayer. Classical molecular dynamics simulations, such as those described here, calculate atomic forces on each atom resulting from their interactions as governed by the integration of the equations of motion for every atom over some time period (*35*). The forces on the atoms are computed from interaction potentials, including both intra- and intermolecular contributions, commonly denoted as force fields. An all-atom molecular representation was used for the catechins, lipids, and water, with the exception of the lipid hydrocarbon tails, which were treated with a united-atom model. Intramolecular interactions for the lipids and nonbonded interactions (Lennard−Jones and Coulombic potentials) were the same as those from a previous study (*36*). The single point charge (SPC) model was used for water (*37*). The OPLS (optimized potential for liquid simulations) force field (*38*), a widely used force field for organic compounds, was employed for all catechins compounds.

Molecular dynamics simulations were performed using the leapfrog integration scheme with a time step of 2 fs (femtosecond = $10^{-15}$ s). Short-range van der Waals and electrostatic interactions were cut off at 0.9 nm. The particle mesh Ewald (PME) method was used to correct for long-range electrostatic interactions (*39, 40*). The LINear Constraint Solver (LINCS) algorithm (*41*) was applied to constrain all bonds in the lipids and catechins and the SETTLE algorithm (*42*) for the water molecules. Periodic boundary conditions were applied in all directions. All simulations were performed in the NPT ensemble using the Berendsen weak coupling technique and anisotropic pressure scaling

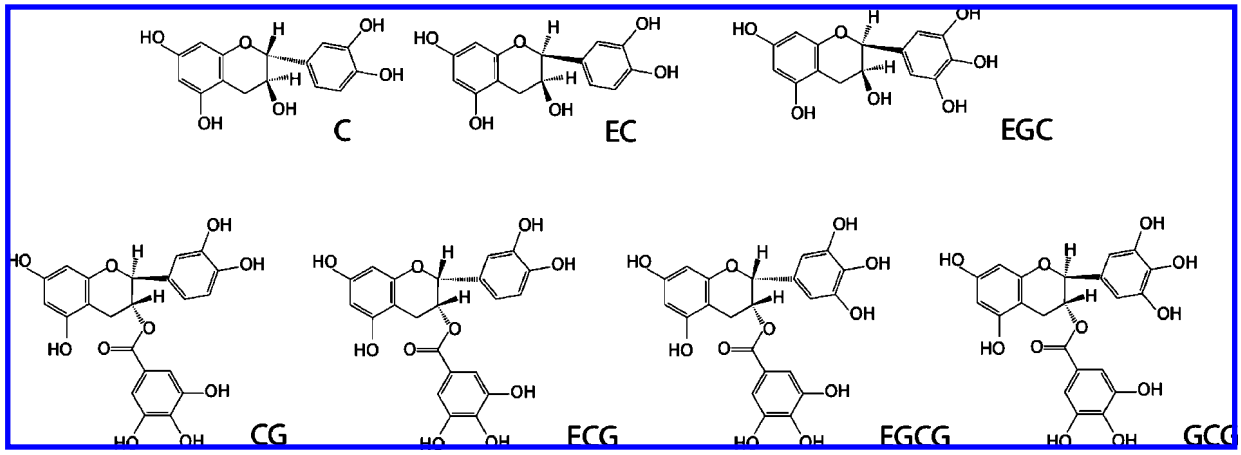


**Figure 1.** Molecular structures for the following catechins commonly found in green and black teas: C, EC, EGC, CG, ECG, EGCG, and GCG.

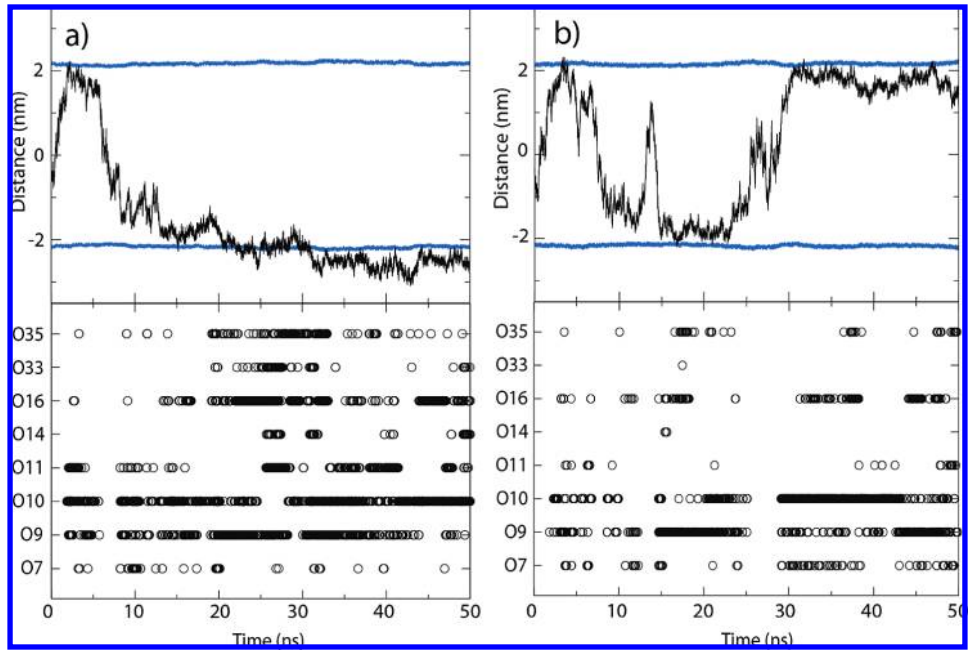


**Figure 2.** Top portion of the figure shows the COM molecular trajectory for (**a**) catechin (C) and (**b**) epigallocatechin (EGC). The solid blue lines represent the average position of the phosphorus atoms in the PC and PE headgroups. Position zero corresponds to the middle of the aqueous phase. Regions above and below the solid blue lines correspond to the lipid bilayer. Because of periodic boundary conditions, the catechins can interact with either bilayer surface. The bottom portion of the figure shows the hydrogen bonding of the catechins with the respective lipid oxygen atom (see **Figure 5** for labeling) over the course of the simulation.

(*43*). The GROMACS 3.3.1 software package (single precision) (*44*−*46*) was used for all simulations running in parallel on Virginia Tech's System X.

The systems studied were comprised of catechins interacting with a model cell membrane, which had a lipid composition representative to that of HepG2 liver cancer cells. The two major fatty acids (lipid tails) found in liver cells are saturated C16 (50% by weight) and monounsaturated C18 (35%) (*47*). The lipid composition of HepG2 cells is about 75% of PC (phosphatidylcholine) and PE (phosphatidylethanolamine) with six other lipids making up the remaining 25% (*48*). Therefore, as an approximation for HepG2 cells, we considered lipid bilayers containing a 1:1 mixture of 1-palmitoyl-2-oleoyl-phosphatidylcholine (POPC) and 1-palmitoyl-2-oleoyl-phosphatidylethanolamine (POPE).

The 1:1 POPC:POPE bilayers contained 144 lipids per leaflet. The lipid bilayers were built by randomly placing the lipids (72 POPC and 72 POPE) on a grid to form a monolayer. This monolayer was combined with another monolayer to form a bilayer structure. A total of 11520 water molecules (40 water/lipid) were added to the lipid bilayer to create a fully hydrated system. The system was initially heated to 450 K for 10 ns, then cooled, and equilibrated at 310 K for 50 ns. The resulting configuration was used for simulations with the test compounds, which were inserted into the center of the aqueous phase.

Structural and dynamic properties for the seven catechins with the lipid bilayers, such as molecular orientation and hydrogen bonding, were monitored during 50 ns (nanosecond) simulations by examining the molecular trajectory saved every 2 ps. All simulations were performed at 310 K and 1 bar, corresponding to a liquid-crystalline state for the mixed POPC:POPE bilayer (see ref *36* for details). The stability of the equilibrated bilayer was confirmed from the area per lipid (lipid bilayer area divided by the number of lipids per leaflet), which was found to be 0.57 $nm^2$, and the lipid tail order parameter. Both quantities were in agreement with previously reported values for POPC/POPE bilayers (*36*). Detailed information regarding the properties of the mixed POPC/POPE lipid bilayer can be found elsewhere (*36*).

## RESULTS AND DISCUSSION

**Figure 2** shows the center-of-mass (COM) molecular trajectories for C and EGC, which are representative of the catechins considered here (see Supporting Information for the molecular trajectory of the other catechins). The trajectories illustrate two

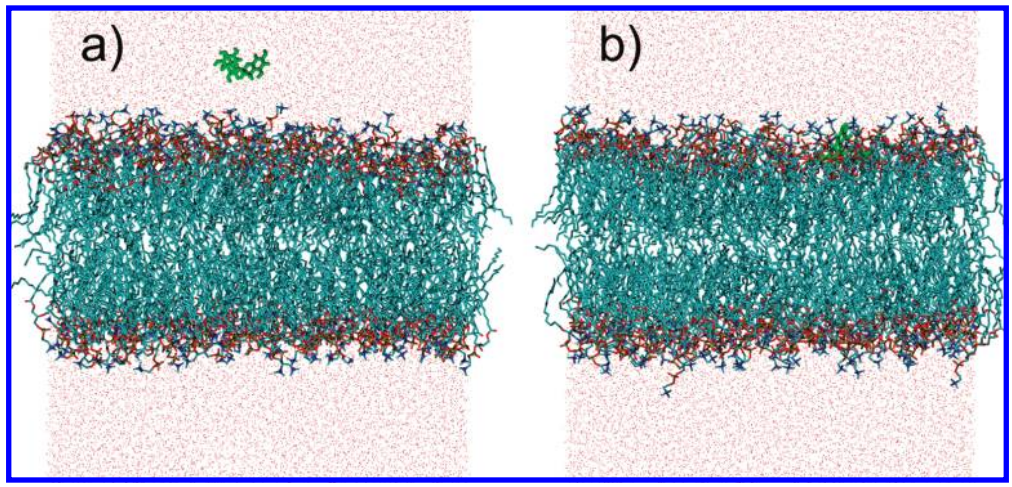


**Figure 3.** Snapshots of the lipid bilayers (center of figures) with EGCG (blue) (**a**) initially in the aqueous phase and (**b**) after diffusion to bind to the bilayer surface. The system is periodic in all directions, and as such, the aqueous phase is continuous and EGCG can interact with both bilayer surfaces. Red dots correspond to water molecules.

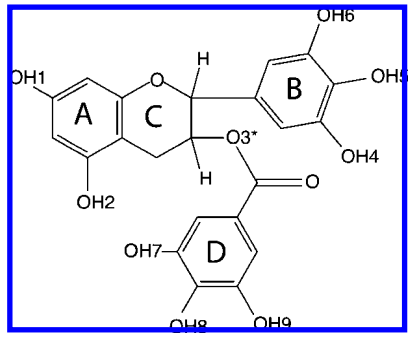


**Figure 4.** Identification of the ring structures and functional groups in the catechins. Phenolic OH donor groups (OH1−OH9) and ring labels (A−D) for catechins are used for reference in the discussions in the text. Note that OH7, OH8, and OH9 are not present in C, EC, and EGC.

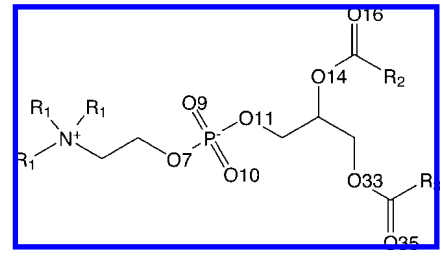


**Figure 5.** Chemical structure of the lipid headgroup and the corresponding oxygen atom numbering assignment: R1 is $CH_3$ and H for the PC and PE lipids, respectively. R2 and R3 are the oleic acid and palmitic acid tails, respectively.

distinct types of catechin−bilayer interactions: (i) binding to the lipid headgroups near the bilayer surface (adsorption) and (ii) penetration into the bilayer interface (absorption). As shown in the figure, the catechins initially inserted in the middle of the aqueous phase and quickly diffused through the aqueous phase to bind to the bilayer surface. All of the catechins interacted with the lipid headgroups: some had predominantly interfacial interactions (EGC, CG, ECG, and GCG adsorbed on the surface), while some penetrated into the bilayer (C, EC, and EGCG absorbed underneath the bilayer surface).

**Figure 3** illustrates one such interaction with snapshots of EGCG initially in the aqueous phase and after diffusion through the aqueous phase to bind to the bilayer surface. A distinctive molecular feature of all catechins that only adsorbed on the bilayer surface is the presence of the gallate ester moiety, with the exception of EGC (the gallate moiety is represented by ring D in **Figure 4**). Two catechins (C and EC) that were absorbed into the bilayer did not have the gallate moiety. The dynamics of EGCG were unique relative to the other catechins. It fluctuated between being adsorbed on and absorbed into the bilayer surface. It is also worthwhile to note that although C, EC, and EGC are structurally similar, EGC was unable to penetrate the bilayer surface (EC and EGC differ by one phenolic OH group in ring B—see **Figure 4**). These results suggest that chemical functionality and stereochemistry govern interactions with the lipid bilayer.

A detailed analysis of the hydrogen bonding between the catechins and the lipids was performed to better understand the interactions along the bilayer interface. A hydrogen bond was defined as the distance between the H-donor and the H-acceptor of less than 0.35 nm and a donor−hydrogen−acceptor angle between 120 and 180° (*49*). This analysis considered two cases: (i) catechin phenolic OH groups as H-donors and lipid oxygen groups as H-acceptors and (ii) ethanolamine groups in POPE as H-donors and catechin oxygen atoms as H-acceptors. The lower portion of the plots in **Figure 2** shows the hydrogen bonding of the phenolic OH groups (H-donor) in the catechins to the lipid oxygen atoms (H-acceptor—see **Figure 5** for naming assignment of the oxygen atoms of the PC and PE headgroups). Monitoring the hydrogen bonds formed along the catechin trajectories provides insight into the interactions between the catechin and the lipids as the catechins approach to and then bond to the bilayer surface. Catechins penetrating into the lipid bilayer showed predominant interactions with the lipid oxygen atoms further away from the bilayer surface (O16, O33, and O35), whereas those that remained adsorbed on the bilayer surface predominately formed hydrogen bonds with the phosphate oxygen atoms (O7, O9, and O10). Note that the COM position is not a definitive measure of the penetration of the catechins into the bilayer, as parts of the molecule can be relatively far from the COM depending on their configuration and orientation. This may be the reason why hydrogen bonds can be found even though the COM position seems relatively distant from the bilayer surface. In addition, the PE headgroups are often at a lower position in the bilayer than the PC headgroups, allowing the catechin molecules to enter voids

**Table 1.** Distribution of Hydrogen Bonds Formed among the Catechin Phenolic OH Donor Groups (H-Donor) with Lipid Oxygen Atoms (H-Acceptor)[a]

| | C | EC | EGC | CG | ECG | EGCG | GCG |
|---|---|---|---|---|---|---|---|
| OH1 | 7224 (25) | 2009 (7) | 1627 (9) | 4669 (12) | 623 (6) | 3947 (9) | 2891 (9) |
| OH2 | 6294 (22) | 9625 (32) | 6789 (38) | 11060 (28) | 1338 (14) | 4215 (9) | 1877 (6) |
| OH3 | 1243 (4) | 4372 (15) | 2000 (11) | | | | |
| OH4 | | | 3078 (17) | | | 744 (2) | 5709 (17) |
| OH5 | 4277 (15) | 6703 (23) | 2558 (14) | 2838 (7) | 1526 (15) | 6721 (15) | 4444 (13) |
| OH6 | 9574 (34) | 6962 (23) | 1941 (11) | 3200 (8) | 944 (10) | 10113 (22) | 2801 (8) |
| OH7 | | | | 5065 (13) | 1173 (12) | 2517 (6) | 5153 (15) |
| OH8 | | | | 6373 (16) | 2088 (21) | 3514 (8) | 6633 (20) |
| OH9 | | | | 6640 (17) | 2138 (22) | 13088 (29) | 4167 (12) |
| total | 28612 | 29671 | 17993 | 39845 | 9830 | 44859 | 33675 |

[a] Hydrogen bonds were accumulated over the 50 ns of simulation time. The total hydrogen bonds formed are shown in the last row. Numbers in parentheses are a percentage of the total.

above the PE headgroups, where they can interact with nearby oxygen atoms in the PC headgroups.

The number and characteristics of the catechin−lipid hydrogen bonds were examined closely. **Table 1** shows the frequency of hydrogen bonds formed for each catechin and the distribution of hydrogen bonds among the catechin donor groups. These results indicate that the presence of the gallate moiety was especially important, as catechins with the gallate moiety formed about 40% more hydrogen bonds than did those without the side chain. ECG was an exception. It formed about one-third less hydrogen bonds than did the corresponding structure without the gallate moiety (EC). ECG had the least number of hydrogen bonds formed with the lipid bilayer. Catechins that absorbed into and penetrated the bilayer (C and EC) formed more hydrogen bonds with lipid oxygen atoms deeper in the bilayer surface (O14, O33, and O35). The catechins were overwhelmingly H-donors rather than H-acceptors in all systems and in all hydrogen bonds formed. The catechins without the gallate moiety (C, EC, and EGC) showed a stronger preference to form hydrogen bonds on ring A, whereas most of the hydrogen bonds formed by compounds with the gallate moiety were on rings B and D. EGCG had the most interactions with the lipid bilayer, with hydrogen bonds formed by the phenolic OH6 and OH9 groups accounting for about 51% of the total.

Among the catechins without the gallate moiety, EGC formed the least number of hydrogen bonds, despite having one more donor site in ring C as compared to C and EC. When EGC bonded to the bilayer, about 72% of the interactions resulted from only one hydrogen bond as compared to about 40 and 53% for EC and C, respectively. EC was observed to form the highest number of hydrogen bonds among catechins without the gallate moiety. Like most other catechins in a *cis* configuration, it was more likely to form several multiple hydrogen bonds than was the case with the *trans* stereoisomer (C). **Table 2** summarizes the number of multiple hydrogen bonding formed by each catechin.

The mobility of each compound substantially decreased after binding to the bilayer. **Figure 6** shows the trajectory for one of the catechins (C) as it diffused along the plane parallel to the bilayer surface (the molecules were allowed to move in all directions; the trajectory shown only captures the displacement along the *xy*-plane). The figure shows that in the first 13 ns, the flavonoid exhibits significant mobility, transversing an area of approximately 9.0 nm$^2$. It then adsorbed onto the bilayer surface and remained bounded thereafter until the end of the simulation (confirmed from the COM trajectory and hydrogen bonding data—see **Figure 2**). Once bound to the bilayer surface, the motion of the flavonoid was localized, covering only about 3.0

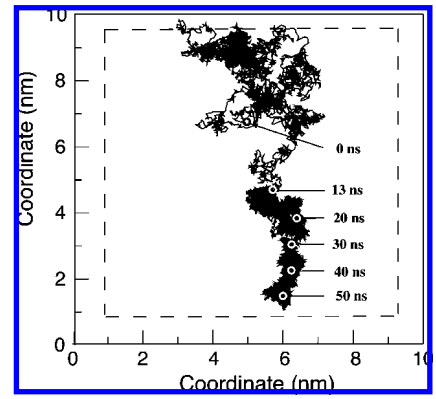


**Figure 6.** Representative molecular trajectory of catechin (C) along the plane (*xy*) parallel to the bilayer surface. Marked locations with times correspond to the COM position shown in **Figure 2**. The molecule diffuses in the aqueous phase during the first 13 ns, at which point it is adsorbed on the bilayer surface. At 30 ns, it is absorbed into the bilayer. The dashed line indicates the simulation box boundaries.

nm$^2$ in 37 ns. A similar loss of mobility was observed for EC after it bounded to the bilayer surface. The catechins adsorbed to the bilayer surface showed relatively greater mobility along the surface than those absorbed into the bilayer, presumably because in the latter case, the molecules were enclosed by the lipid headgroups.

The configuration of the catechins on the bilayer surface may be an important factor impacting their bioactivity. To understand the conformation of each molecule once bound to the bilayer surface, the angle of intersection between the plane of each molecular ring and the plane of the bilayer surface (*xy*-plane) was measured for those instances in which the catechins were hydrogen bonded to the bilayer. **Figure 7** shows the angle distributions for the rings shown in **Figure 4**. These results show no preferential orientation in the angle distributions. This conclusion was verified through visualization of the molecular trajectories. However, some trends were identified in the angle distributions. For most of the catechins, rings B and D preferred to form an angle >50° with the bilayer surface, as seen in the broad angle distributions in **Figure 7**. Ring A of GCG, ECG, EGC, and EC showed preference for angles >60° with the bilayer surface, while ring A of C, CG, and EGCG was more likely to be oriented at ∼40°. None of the rings showed a preferred parallel orientation with the bilayer surface.

**Table 2** shows that EGCG has a unique ability to form multiple H-bonds. To further understand these interactions, we examined the angle distribution for each ring in EGCG relatively to the bilayer surface for those instances when one or more hydrogen bonds were formed. **Figure 8b**,**c** shows that rings B and D of EGCG approximately maintained the orientation regardless of the number of hydrogen bonds formed. The orientation of ring A/C was also very similar and was independent of the number of hydrogen bonds formed. However, there was a slight shift to lower angles when three or more hydrogen bonds were present. The figure also shows that ring D preferentially bounded to the bilayer surface at angles between about 40 and 60° and that ring B was more favorably located in an almost normal orientation to the surface.

The angle distributions for EGCG were compared to CG, a closely rated catechin. **Table 2** shows that CG did not form multiple hydrogen bonds as frequently but did have a similar number of interactions with the bilayer. In contrast to EGCG, the orientation for ring A in CG became more parallel to the bilayer surface as multiple hydrogen bonds were formed and

**Table 2.** Number of Occurrences for Single and Multiple Hydrogen Bonds Formed by Catechins[a]

| H-bonds | C | EC | EGC | CG | ECG | EGCG[b] | GCG |
|---|---|---|---|---|---|---|---|
| 1 | 9449 (53) | 6501 (40) | 10005 (72) | 6609 (35) | 3449 (58) | 3918 (23) | 5787 (33) |
| 2 | 6060 (34) | 6462 (40) | 3527 (26) | 6334 (33) | 1600 (27) | 4669 (27) | 7385 (43) |
| 3 | 2197 (12) | 2595 (16) | 278 (2) | 4228 (22) | 670 (11) | 4516 (26) | 3551 (21) |
| 4 | 113 (1) | 604 (4) | 25 (0) | 1729 (9) | 269 (4) | 2828 (16) | 595 (3) |
| 5 | 0 | 9 (0) | 0 | 184 (1) | 19 (0) | 1203 (7) | 17 (0) |
| total 2+ | 8370 (47) | 9670 (60) | 3830 (28) | 12475 (65) | 2558 (43) | 13336 (77) | 11548 (67) |
| total | 17819 | 16171 | 13835 | 19084 | 6007 | 17254 | 17335 |

[a] Numbers in parentheses correspond to the percentage of the total. Results for catechins forming more than six hydrogen bonds are not shown, as they represent an insignificant percentage. The total number of multiple hydrogen bonds is shown in the second to the last row. [b] Six and seven hydrogen bonds accounted for the remaining 1%.

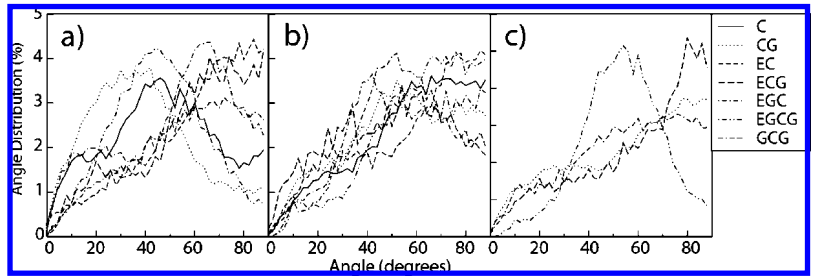


**Figure 7.** Normalized angle distribution for the plane of the molecular ring in the catechins relative to the bilayer surface. Lines correspond to the angle distribution for (**a**) ring A/C, (**b**) ring B, and (**c**) ring D for each catechin. Angles were measured only at the instances that the molecules formed at least one hydrogen bond with the bilayer surface.

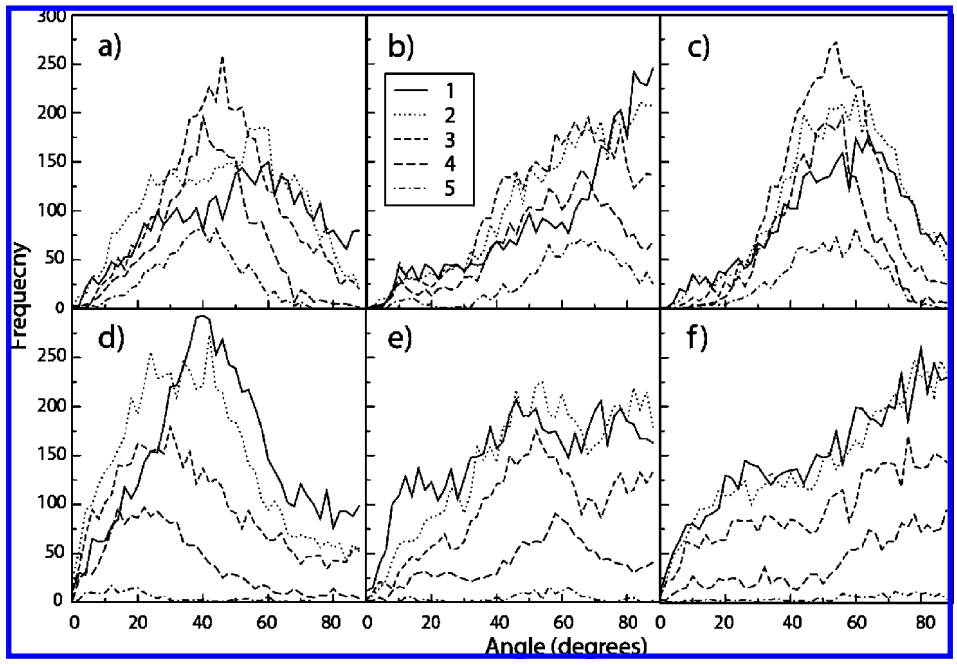


**Figure 8.** Top: Angle distributions for EGCG (**a**) ring A/C, (**b**) ring B, and (**c**) ring D. Each line represents the case of one, two, three, four, or five simultaneous hydrogen bonds as shown in the legend. The peaks of the angle distributions for the case of one or two simultaneous hydrogen bonds are similar for each ring. This is also true for the case of three or more simultaneous hydrogen bonds. Bottom: Angle distributions for CG (**d**) ring A/C, (**e**) ring B, and (**f**) ring D. Each additional hydrogen bond of CG with the bilayer influences rings A/C and B to form angles approximately 5° larger and smaller, respectively, with the bilayer. Note that for CG, the frequency of simultaneous hydrogen bonding decreases as the number of hydrogen bonds increases.

the orientation for ring B was more defined, peaking between 40 and 60°. EGCG was also unique because a large fraction of its interactions with the lipid bilayer resulted from the formation of two hydrogen bonds. By contrast, either one or about equally one and two hydrogen bonds were dominant for the other catechins (see **Table 2** for details).

The ability of EGCG to form multiple hydrogen bonds without a substantial change in structural conformation may explain both the large number of hydrogen bonds formed and its unique ability to form multiple hydrogen bonds. For example, GCG, a stereoisomer of EGCG, forms substantially less total hydrogen bonds (see **Table 1**) and multiple hydrogen bonds (see **Table 2**) as compared to EGCG. These observations suggest that the phenolic OH4 group in EGCG and GCG significantly affects the interactions of the catechins with the lipid bilayer.

Another characteristic observed is that the catechins with the O3* group in a *cis* configuration relative to ring B (EC, EGC, ECG, and EGCG), again with the exception of ECG, formed

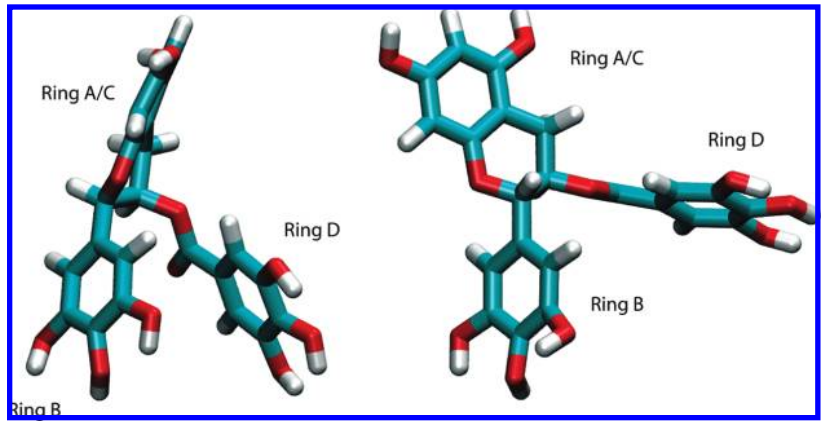


**Figure 9.** Typical molecular configurations for (**a**) EGCG and (**b**) GCG. Phenolic OH groups in rings B and D for EGCG are parallel and in close proximity, whereas those for GCG are farther apart.

more multiple hydrogen bonds as compared to their respective stereoisomer with the O3* group in a *trans* configuration (C, CG, and GCG) (see **Table 2** for details). Catechins with the O3* group in a *cis* configuration resulted in a close placement of rings B and D. By contrast, **Figure 9** shows that these rings were farther apart for catechins with a *trans* configuration. The nearby placement and orientation of the phenolic OH groups in the *cis* configuration may be responsible for the increased formation of multiple hydrogen bonds by rings B and D. In the *trans* configuration (C, CG, and GCG), some phenolic OH groups are oriented away from the bilayer surface when either ring B or D binds, resulting in an unfavorable conformation to allow formation of additional hydrogen bonds. The large number of hydrogen bonds formed by the groups in rings B and D of EGCG support this conclusion, as do the findings that its stereoisomer (GCG) formed fewer multiple hydrogen bonds and that EGCG had a more uniform distribution of hydrogen bonds among all of the phenolic OH groups. ECG, a catechin similar to EGCG, had limited interactions with the lipid bilayer in the simulation performed. It is unclear whether it can form multiple hydrogen bonds as do the other catechins. This observation suggests that the stereochemistry of catechins influences the affinity to membranes.

## SIGNIFICANCE FOR CATECHIN CELL MEMBRANE INTERACTIONS

We presented results from molecular dynamics simulations on the interactions of seven tea catechins with a mixed POPC/POPE bilayer. To our knowledge, this is the first molecular level study to examine the dynamics and binding of catechins with lipid bilayers to facilitate understanding of the contribution of hydrogen-bonding effects to their role as bioactive agents. All catechins considered demonstrated affinity for the lipid bilayer surface, including three that were absorbed underneath the bilayer surface. Experimental studies have suggested that catechins may be absorbed into and diffused through the cell membrane (*27*). Despite the relatively short duration of our simulations (50 ns), we observed that some catechins (C, EC, and EGCG) were nevertheless incorporated into the lipid bilayer. The time required for absorption into the bilayer is related to the size and functional properties of the molecules.

The dynamics of the catechins along or inside the bilayer surface may influence bioactivity in cells. As the catechins bounded to the bilayer surface, they remained mobile (diffused along the bilayer surface) and flexible (changed structural conformation). The diffusion of the catechins along the bilayer surface was characterized by the formation and breaking of hydrogen bonds with the lipid headgroups. For the catechins that were absorbed into the bilayer, their displacement within the bilayer was significantly restricted. They were essentially trapped between the lipid molecules. Their ability to migrate over the bilayer surface and their eventual penetration to the bilayer may be potentially linked to the mechanism for apoptosis and other biological effects involving cell membranes.

The frequency of hydrogen bonds between the catechins and the lipid bilayer was uncorrelated to the number of hydrogen donor groups in the catechins. Among the compounds without the gallate moiety, EGC formed relatively fewer hydrogen bonds (remained mostly in the aqueous phase) with the lipid bilayer than did similar catechins (C and EC). This observation is in agreement with the experimental study by Hashimoto et al. (*50*). These authors found that EGC has the lowest affinity for liposomes as compared to EC, ECG, and EGCG and that the additional phenolic OH4 group in ring B in EGC lowers its hydrophobicity as compared to EC and ECG.

EGCG is one of the most studied catechins in cancer research, because of both its high concentrations in tea and its potential health benefits. Our results show that it readily forms hydrogen bonds with the lipid bilayer. EGCG formed the most total number of hydrogen bonds (see **Table 1**) and the most number of multiple hydrogen bonds (from **Table 2**, two or more H-bonds accounted for 77% of H-bonds formed) with the lipid bilayer. Our simulations indicate that the presence of the gallate moiety in EGCG and its *cis* configuration with ring B both facilitate the formation of multiple hydrogen bonds. EGCG's unique ability to form hydrogen bonds with the lipid bilayer may be closely related to its ability to target specific cells. Such bonds potentially alter charge distributions both on the surface and within the membranes, resulting in loss of cell viability. Our results provide mechanistic insight into the binding of catechins to lipid membranes, in particular in light of recent experimental studies reporting that EGCG and ECG (catechins with the gallate moiety) have a much larger affinity (about 1000 times greater) for lipid bilayers than EC and EGC (*51*). Just as in our results, the experimental measurements identified EGCG to strongly bind to the lipid membrane, which results from the large number of hydrogen bonds formed.

The results of the present study complement and extend the cited observation on catechin−cell membrane interactions that may govern mechanisms of health-promoting effects of catechins. The described findings are not only of fundamental interest but also have practical implications for plant and food sciences and human health. Results of ongoing studies on effects

of multiple catechins, including interactions with other phospholipids of cell membranes, will be examined in a future publication.

## ACKNOWLEDGMENT

Computational resources were provided by the Virginia Tech Advanced Research Computing Facility (System X).

**Supporting Information Available:** Trajectories of the catechins along the normal direction and parallel plane to the bilayer surface. This material is available free of charge via the Internet at http://pubs.acs.org.

## LITERATURE CITED

(1) Sutherland, B. A.; Rahman, R. M.; Appleton, I. Mechanisms of action of green tea catechins, with a focus on ischemia-induced neurodegeneration. *J. Nutr. Biochem.* **2006**, *17* (5), 291–306.

(2) Zaveri, N. T. Green tea and its polyphenolic catechins: medicinal uses in cancer and noncancer applications. *Life Sci.* **2006**, *78* (18), 2073–2080.

(3) Juneja, V. K.; Bari, M. L.; Inatsu, Y.; Kawamoto, S.; Friedman, M. Control of *Clostridium perfringens* spores by green tea leaf extracts during cooling of cooked ground beef, chicken, and pork. *J. Food Prot.* **2007**, *70* (6), 1429–1433.

(4) Friedman, M.; Henika, P. R.; Levin, C. E.; Mandrell, R. E.; Kozukue, N. Antimicrobial activities of tea catechins and theaflavins and tea extracts against *Bacillus cereus*. *J. Food Prot.* **2006**, *69* (2), 354–361.

(5) Friedman, M.; Mackey, B. E.; Kim, H. J.; Lee, I. S.; Lee, K. R.; Lee, S. U.; Kozukue, E.; Kozukue, N. Structure−activity relationships of tea compounds against human cancer cells. *J. Agric. Food Chem.* **2007**, *55* (2), 243–253.

(6) Tang, S. Z.; Ou, S. Y.; Huang, X. S.; Li, W.; Kerry, J. P.; Buckley, D. J. Effects of added tea catechins on colour stability and lipid oxidation in minced beef patties held under aerobic and modified atmospheric packaging conditions. *J. Food Eng.* **2006**, *77* (2), 248–253.

(7) Bañón, S.; Díaz, P.; Rodríguez, M.; Garrido, M. D.; Price, A. Ascorbate, green tea and grape seed extracts increase the shelf life of low sulphite beef patties. *Meat Sci.* **2007**, *77* (4), 626–633.

(8) O'Grady, M. N.; Maher, M.; Troy, D. J.; Moloney, A. P.; Kerry, J. P. An assessment of dietary supplementation with tea catechins and rosemary extract on the quality of fresh beef. *Meat Sci.* **2006**, *73* (1), 132–143.

(9) Mitsumoto, M.; O'Grady, M. N.; Kerry, J. P.; Joe Buckley, D. Addition of tea catechins and vitamin C on sensory evaluation, colour and lipid stability during chilled storage in cooked or raw beef and chicken patties. *Meat Sci.* **2005**, *69* (4), 773–779.

(10) Jo, C.; Son, J. H.; Son, C. B.; Byun, M. W. Functional properties of raw and cooked pork patties with added irradiated, freeze-dried green tea leaf extract powder during storage at 4 °C. *Meat Sci.* **2003**, *64* (1), 13–17.

(11) Nissen, L. R.; Byrne, D. V.; Bertelsen, G.; Skibsted, L. H. The antioxidative activity of plant extracts in cooked pork patties as evaluated by descriptive sensory profiling and chemical analysis. *Meat Sci.* **2004**, *68* (3), 485–495.

(12) Weisburger, J. H.; Hara, Y.; Dolan, L.; Luo, F. Q.; Pittman, B.; Zang, E. Tea polyphenols as inhibitors of mutagenicity of major classes of carcinogens. *Mutat. Res.* **1996**, *371* (1−2), 57–63.

(13) Friedman, M.; Kim, S.-Y.; Lee, S.-J.; Han, G.-P.; Han, J.-S.; Lee, R.-K.; Kozukue, N. Distribution of catechins, theaflavins, caffeine, and theobromine in 77 teas consumed in the United States. *J. Food Sci.* **2005**, *70*, C550–C559.

(14) Friedman, M.; Levin, C. E.; Choi, S.-H.; Kozukue, E.; Kozukue, N. HPLC analysis of catechins, theaflavins, and alkaloids in commercial teas and green tea dietary supplements: Comparison of water and 80% ethanol/water extracts. *J. Food Sci.* **2006**, *71*, C328 337.

(15) Weber, A. A.; Neuhaus, T.; Skach, R. A.; Hescheler, J.; Ahn, H. Y.; Schror, K.; Ko, Y.; Sachinidis, A. Mechanisms of the inhibitory effects of epigallocatechin-3 gallate on platelet-derived growth factor-BB-induced cell signaling and mitogenesis. *FASEB J.* **2004**, *18* (1), 128–130.

(16) Zhang, Y. M.; Rock, C. O. Evaluation of epigallocatechin gallate and related plant polyphenols as inhibitors of the FabG and FabI reductases of bacterial type II fatty-acid synthase. *J. Biol. Chem.* **2004**, *279* (30), 30994–31001.

(17) Szewczuk, L. M.; Penning, T. M. Mechanism-based inactivation of COX-1 by red wine m-hydroquinones: A structure−activity relationship study. *J. Nat. Prod.* **2004**, *67* (11), 1777–1782.

(18) Nagle, D. G.; Ferreira, D.; Zhou, Y. D. Epigallocatechin-3-gallate (EGCG): Chemical and biomedical perspectives. *Phytochemistry* **2006**, *67* (17), 1849–1855.

(19) Dobrzynska, I.; Sniecinska, A.; Skrzydlewska, E.; Figaszewski, Z. Green tea modulation of the biochemical and electric properties of rat liver cells that were affected by ethanol and aging. *Cell. Mol. Biol. Lett.* **2004**, *9* (4A), 709–721.

(20) Caturla, N.; Vera-Samper, E.; Villalain, J.; Mateo, C. R.; Micol, V. The relationship between the antioxidant and the antibacterial properties of galloylated catechins and the structure of phospholipid model membranes. *Free Radical Biol. Med.* **2003**, *34* (6), 648–662.

(21) Lozano, C.; Julia, L.; Jimenez, A.; Tourino, S.; Centelles, J. J.; Cascante, M.; Torres, J. L. Electron-transfer capacity of catechin derivatives and influence on the cell cycle and apoptosis in HT29 cells. *FEBS J.* **2006**, *273* (11), 2475–2486.

(22) Uekusa, Y.; Kamihira, M.; Nakayama, T. Dynamic behavior of tea catechins interacting with lipid membranes as determined by NMR spectroscopy. *J. Agric. Food Chem.* **2007**, *55* (24), 9986–9992.

(23) Kajiya, K.; Kumazawa, S.; Naito, A.; Nakayama, T. Solid-state NMR analysis of the orientation and dynamics of epigallocatechin gallate, a green tea polyphenol, incorporated into lipid bilayers. *Magn. Reson. Chem.* **2008**, *46* (2), 174–177.

(24) Kajiya, K.; Kumazawa, S.; Nakayama, T. Effects of external factors on the interaction of tea catechins with lipid bilayers. *Biosci., Biotechnol., Biochem.* **2002**, *66* (11), 2330–2335.

(25) Kajiya, K.; Hojo, H.; Suzuki, M.; Nanjo, F.; Kumazawa, S.; Nakayama, T. Relationship between antibacterial activity of (+)-catechin derivatives and their interaction with a model membrane. *J. Agric. Food Chem.* **2004**, *52* (6), 1514–1519.

(26) Kajiya, K.; Kumazawa, S.; Nakayama, T. Steric effects on interaction of tea catechins with lipid bilayers. *Biosci., Biotechnol., Biochem.* **2001**, *65* (12), 2638–2643.

(27) Kumazawa, S.; Kajiya, K.; Naito, A.; Saito, H.; Tuzi, S.; Tanio, M.; Suzuki, M.; Nanjo, F.; Suzuki, E.; Nakayama, T. Direct evidence of interaction of a green tea polyphenol, epigallocatechin gallate, with lipid bilayers by solid-state nuclear magnetic resonance. *Biosci., Biotechnol., Biochem.* **2004**, *68* (8), 1743–1747.

(28) Wang, X.; Song, K. S.; Guo, Q. X.; Tian, W. X. The galloyl moiety of green tea catechins is the critical structural feature to inhibit fatty-acid synthase. *Biochem. Pharmacol.* **2003**, *66* (10), 2039–2047.

(29) Tamba, Y.; Ohba, S.; Kubota, M.; Yoshioka, H.; Yamazaki, M. Single GUV method reveals interaction of tea catechin (−)-epigallocatechin gallate with lipid membranes. *Biophys. J.* **2007**, *92* (9), 3178–3194.

(30) Rizvi, S. I.; Zaid, M. A. Impairment of sodium pump and Na/H exchanger in erythrocytes from non-insulin dependent diabetes mellitus patients: Effect of tea catechins. *Clin. Chim. Acta* **2005**, *354* (1−2), 59–67.

(31) Takeuchi, Y.; Okuno, K.; Yoshioka, H.; Yoshioka, H. Characteristics of the OH radical scavenging activity of tea catechins. *J. Radioanal. Nucl. Chem.* **2007**, *272* (3), 455–459.

(32) Giacomelli, C.; Miranda Fda, S.; Goncalves, N. S.; Spinelli, A. Antioxidant activity of phenolic and related compounds: A density functional theory study on the O-H bond dissociation enthalpy. *Redox Rep.* **2004**, *9* (5), 263–269.

(33) Friedman, M.; Henika, P. R.; Mandrell, R. E. Antibacterial activities of phenolic benzaldehydes and benzoic acids against *Campylobacter jejuni*, *Escherichia coli* O157:H7, *Listeria monocytogenes*, and *Salmonella enterica*. *J. Food Prot.* **2003**, *66*, 1811–1821.

(34) Medina, I.; Gallardo, J. M.; Gonzalez, M. J.; Lois, S.; Hedges, N. Effect of molecular structure of phenolic families as hydroxycinnamic acids and catechins on their antioxidant effectiveness in minced fish muscle. *J. Agric. Food Chem.* **2007**, *55* (10), 3889–3895.

(35) Frenkel, D.; Smit, B. *Understanding Molecular Simulation: From Algorithms to Applications*; Academic Press: San Diego, 2002.

(36) Leekumjorn, S.; Wu, Y.; Sum, A. K.; Chan, C. Experimental and computational studies investigating trehalose protection of HepG2 cells from palmitate-induced toxicity. *Biophys. J.* **2008**, *94* (7), 2869–2883.

(37) Berendsen, H. J. C.; Postma, J. P. M.; van Gunsteren, W. F.; Hermans, J. In *Intermolecular Forces*, Proc. Fourteenth Jerusalem Symp. Quant. Chem. Biochem., 1981; Pullman, B. Ed.; Reidel: Dordrecht, 1981; pp 331−342.

(38) Jorgensen, W. L.; Maxwell, D. S.; Tirado-Rives, J. Development and testing of the OPLS all-atom force field on conformational energetics and properties of organic liquids. *J. Am. Chem. Soc.* **1996**, *118* (45), 11225–11236.

(39) Darden, T.; York, D.; Pedersen, L. Particle mesh Ewald: An N·log(N) method for Ewald sums in large systems. *J. Chem. Phys.* **1993**, *98* (12), 10089–10092.

(40) Essmann, U.; Perera, L.; Berkowitz, M. L.; Darden, T.; Lee, H.; Pedersen, L. G. A smooth particle mesh Ewald method. *J. Chem. Phys.* **1995**, *103* (19), 8577–8593.

(41) Mazur, A. K. Quasi-Hamiltonian equations of motion for internal coordinate molecular dynamics of polymers. *J. Comput. Chem.* **1997**, *18* (11), 1354–1364.

(42) Miyamoto, S.; Kollman, P. A. SETTLE: An analytical version of the SHAKE and RATTLE algorithms for rigid water models. *J. Comput. Chem.* **1992**, *13*, 952–962.

(43) Berendsen, H. J. C.; Postma, J. P. M.; Van Gunsteren, W. F.; Dinola, A.; Haak, J. R. Molecular dynamics with coupling to an external bath. *J. Chem. Phys.* **1984**, *81* (8), 3684–3690.

(44) Lindahl, E.; Hess, B.; van der Spoel, D. GROMACS: A message-passing parallel molecuar dynamics implementation. *Comput. Phys. Commun.* **1995**, *92*, 43–56.

(45) Lindahl, E.; Hess, B.; van der Spoel, D. GROMACS 3.0: A package for molecular simulation and trajectory analysis. *J. Mol. Model.* **2001**, *7* (8), 306–317.

(46) Van Der Spoel, D.; Lindahl, E.; Hess, B.; Groenhof, G.; Mark, A. E.; Berendsen, H. J. C. GROMACS: Fast, flexible, and free. *J. Comput. Chem.* **2005**, *26* (16), 1701–1718.

(47) de la Maza, M. P.; Hirsch, S.; Nieto, S.; Petermann, M.; Bunout, D. Fatty acid composition of liver total lipids in alcoholic patients with and without liver damage. *Alcohol.: Clin. Exp. Res.* **1996**, *20* (8), 1418–1422.

(48) Koumanov, K. S.; Momchilova-Pankova, A. B.; Wang, S. R.; Infante, R. Membrane phospholipid composition, fluidity and phospholipase A2 activity of human hepatoma cell line HepG2. *Int. J. Biochem.* **1990**, *22* (12), 1453–1455.

(49) Brady, J. W.; Schmidt, R. K. The role of hydrogen-bonding in carbohydrates: molecular dynamics simulations of maltose in aqueous solution. *J. Phys. Chem.* **1993**, *97*, 958–966.

(50) Hashimoto, T.; Kumazawa, S.; Nanjo, F.; Hara, Y.; Nakayama, T. Interaction of tea catechins with lipid bilayers investigated with liposome systems. *Biosci., Biotechnol., Biochem.* **1999**, *63* (12), 2252–2255.

(51) Kamihira, M.; Nakazawa, H.; Kira, A.; Mizutani, Y.; Nakamura, M.; Nakayama, T. Interaction of tea catechins with lipid bilayers investigated by a quartz-crystal microbalance analysis. *Biosci., Biotechnol., Biochem.* **2008**, *72* (5), 1372–1375.

**Received for review April 28, 2008. Revised manuscript received June 24, 2008. Accepted July 2, 2008. T.W.S. acknowledges the financial support provided by the Virginia Tech College of Engineering Dean's Graduate Teaching Fellowship.**

JF8013298